ORIGINAL ARTICLE

In silico Analysis of Marine-Derived Phlorotannins for their Potential Against Critical Inflammatory Cytokines

Manoj Kumar Karuppan Perumal[1], Manikandan Alagumuthu[2], Remya Rajan Renuka[1], Suresh Kumar Subbiah[1]

[1] Centre for Stem cell Mediated Advanced Research Therapeutics, Saveetha Dental College and Hospitals, Saveetha Institute of Medical and Technical Sciences, Saveetha University, Chennai, 600 077, Tamil Nadu, India.
[2] Department of Microbiology, Saveetha Medical College and Hospitals, Saveetha Institute of Medical and Technical Sciences, Chennai-602105, Tamil Nadu, India.

ABSTRACT

Introduction: Cytokines are mediators of inflammation, which is a central biological process of most chronic and degenerative diseases. Inflammatory proteins are also useful therapeutic targets since their dysregulation is a contributor to the pathogenesis of several diseases. Phlorotannins (PTs) are marine derived and are brown algae, which has attracted attention due to their possible anti-inflammatory properties. **Methods:** The therapeutic potentials of six PT subclasses, i.e. tetraphlorethols (C1), phlorethols (C2), fucophloethols (C3), pentaphloethol (C4), fucols (C5), and eckols (C6) against key inflammatory mediators were assessed *in silico* using computational tools. Molecular docking has been done to find binding affinities and interaction profiles. The drug-likeness and pharmacokinetic properties were evaluated using the ADMET (Absorption, Distribution, Metabolism, Excretion) analysis. Time dependence of the stability of the interaction between the ligand and the protein was determined through molecular dynamics (MD) simulations. **Results:** C4 has shown the best binding affinities to the markers of inflammation of tested compounds. It had strong and stable interaction with NF- kB and COX-2 proteins. ADMET profiling indicated that C4 possessed favourable drug-like characteristics such as good solubility, permeability. The stability of C4 protein complexes was also observed by the MD simulation for 200 nanoseconds. **Conclusion:** The study shows that pentaphloethol is a promising anti-inflammatory compound among other PTs. It has an excellent pharmacokinetic profile and stable interactions with cytokine targets. These results indicate that it has therapeutic lead potential in the management of inflammatory diseases.
Malaysian Journal of Medicine and Health Sciences (2025) 21(SUPP13):108-118. doi:10.47836/mjmhs.21.s13.16

Keywords: Molecular docking; Cytokines; ADMET; Marine bioactives; Molecular dynamics

Corresponding Author:
Remya Rajan Renuka, PhD
Email: remya.praveen5@gmail.com
Tel : +91 9442302777

INTRODUCTION

Inflammation, a biological response that plays a central role in homeostasis maintenance and protection of the body against injurious stimuli, including pathogens, injured cells, or irritants. However, dysregulated inflammation leads to acute problems and contributing factors in the various pathological conditions, including cardiovascular disorders, neurodegenerative conditions, autoimmune diseases, and degenerative musculoskeletal disorders (1). The complex mechanisms involved in inflammatory activities range from cellular metabolic processes to intricate systemic responses. Chronic inflammatory diseases, especially those related to the musculoskeletal system, are a growing global health burden with tremendous socioeconomic implications (2).

Pro-inflammatory cytokines are key organizers of the inflammatory response, and their dysregulation has been involved in the pathogenesis of many chronic diseases, which have made them a targeted therapy (3). The major molecular mediators on the inflammatory cascade are the main signalling proteins and cytokines which control the activation of immune cells, the production of inflammatory mediators (4). Nuclear factor kappa-B (NF-κB) is a master transcriptional regulator, which regulates the expression of many inflammatory genes to a variety of stimuli (5). Cyclooxygenase-2 (COX-2) is an inducible enzyme whose synthesis of the prostaglandin, which enhances the effects of inflammation and leads to pain and fever reactions (6). Nuclear Factor kappa-B (NF-κB) is one of the most notable of the cytokine family, which is a pleiotropic pro-inflammatory cytokine that is involved in systemic inflammation, the regulation of immune

cells, and the indication of apoptosis (7). Likewise, interleukins, including IL-1B, IL-6, and IL-8, are central to the process of spreading inflammatory cascades and recruiting immune cells to the location of inflammation as well as maintaining chronic inflammatory conditions (8). Moreover, matrix metalloproteinases (MMPs) are also involved in tissue remodelling and degradation of extracellular matrix that is pathologic in case of chronic inflammatory disorders (9). The joint development of these inflammatory agents forms a self-perpetuating cycle that, when not controlled, results in tissue damage and the development of chronic diseases.

The existing treatment approaches to anti-inflammatory focus mainly on the non-steroidal anti-inflammatory drugs (NSAIDs), corticosteroids, and biological agents that address the individual inflammatory pathways (10–12). These conventional methods are effective in relieving the symptoms, but are linked to a high level of restrictions. NSAIDs are commonly used but are associated with the risks of gastrointestinal complications, cardiovascular events, renal toxicity (13). Despite their high anti-inflammatory action, corticosteroids may cause such undesirable effects as immunosuppression, decrease in bone density, metabolism, and predisposition to infections (14). Specific cytokine biological agents though effective are expensive, they have to be administered orally and can also aggravate the risks of infections because of their immunomodulatory properties (15). Moreover, the resistance of the treatment and the limited understanding of the individual patient reactions to these drugs introduces the necessity of new anti-inflammatory drugs with better safety profiles and multi-drug mechanisms of action (16).

Natural bioactive compounds have shown promise as novel anti-inflammatory therapy with relatively fewer side effects in recent years. Among such marine-derived polyphenolic compounds, especially from the brown alga (Phaeophyceae) phlorotannins (PTs) have emerged to be significant due to their unique molecular structures and resultant potent biological activity (17–19). PTs are a diverse group of compounds, which include tetraphlorethols (C1), phlorethols (C2), fucophloethols (C3), pentaphloethol (C4), fucols (C5), and eckols (C6). Each of these has its unique way of interacting with the inflammatory pathways involved in OA. Numerous studies have shown that these compounds can significantly influence important inflammatory mediators, like NF-κB, COX-2, TNF-α, and MMPs, thereby providing a promising avenue for therapeutic intervention (20,21). Despite the encouraging preclinical results, the specific molecular relationships between various PT subtypes and the essential inflammatory proteins involved in the pathophysiology of OA remain poorly understood. Additionally, the comparative efficacy of these natural compounds against established anti-inflammatory drugs remains largely unexplored, limiting their potential clinical application. Recent in vitro and in vivo findings indicate that PTs have the capability of regulating several inflammatory pathways, possibly having significant potential compared to conventional drugs that only target single pathways (22,23). The multi-target approaches of PTs make them promising drug in the development of novel anti-inflammatory therapeutics. Nevertheless, even with promising preclinical results, the mechanisms of action at the molecular level between various PT subtypes and essential inflammatory proteins are still largely unknown (24). The structure-activity relationship determining the affinity of PT binding and specificity to different inflammatory targets is suboptimal. Moreover, the comparative effects of these natural compounds with proven anti-inflammatory medications have not been systematically studied, which inhibits to determine the promising therapeutic potential and prioritize specific PT structures for further development.

Computational approaches, particularly molecular docking, pharmacokinetic predictions, and molecular dynamics (MD) simulations, have become indispensable tools in modern drug discovery, enabling the rational identification and optimization of lead compounds before costly experimental validation (25). These *in silico* methodologies allow researchers to predict binding modes, estimate binding affinities, assess drug-likeness properties, and evaluate the stability of protein-ligand complexes under physiological conditions. When applied to natural product research, these computational tools can accelerate the identification of promising bioactive compounds from complex mixtures and provide mechanistic insights into their modes of action (26). This study aims to comprehensively evaluate the anti-inflammatory potential of marine-derived phlorotannins through an integrative computational investigation combining molecular docking, ADMET predictions, and MD simulations. By systematically examining the interactions between diverse PTs subtypes and critical inflammatory proteins. we seek to identify lead phlorotannin compounds with superior binding characteristics and favourable pharmacokinetic profiles. This integrative computational approach not only enhances our fundamental understanding of PT molecular mechanisms but also provides a rational foundation for prioritizing specific compounds for experimental validation and potential development as next-generation anti-inflammatory therapeutics.

MATERIALS AND METHODS

Molecular docking analysis

Protein preparation, ligand preparation, and molecular docking were the three main phases (27–29). The PDB structures of the target protein were retrieved from RCSB (www.rcsb.org/). X-ray crystal 3D structure of the target proteins that are involved in inflammation pathways Cyclooxygenase-2 (COX-2; PDB ID: 1CX2), Tumor Necrosis Factor-α (TNF-α; PDB ID: 2AZ5), Interleukin-8

(IL-8; PDB ID: 3IL8), Nuclear Factor kappa-B (NF-κB; PDB ID: 4DN5), Interleukin-1β (IL-1β; PDB ID: 7CHY), and Interleukin-6 (IL-6; PDB ID: 8C3U) were retrieved. All protein structures were prepared by removing water molecules, co-crystallised ligands, and other heteroatoms. Polar hydrogen atoms were added, and Gasteiger charges were computed using AutoDock Tools (version 1.5.6) to prepare the proteins for docking simulations. Energy minimization for all proteins was carried out in both UCSF Chimera (https://www.cgl.ucsf.edu/chimera/) and BIOVIA Discovery Studio Visualizer software (www.3ds.com/products/biovia/discovery-studio). During the energy minimisation process, except for the target protein chain, all remaining structures, including ligands and water molecules, were deleted (30,31). The ligands used in this study were designed and drawn using ChemDraw. Briefly, the 2D chemical structures drawn in ChemDraw were saved in MOL format and imported into ArgusLab software for 3D structure generation (http://www.arguslab.com/arguslab.com/Welcome.html).

The structures were converted into 3D conformations and energy minimization was performed using Arguslab built-in molecular mechanics methods to obtain the most stable low-energy conformations. The optimized 3D structures were then exported and further processed using Open Babel (https://openbabel.org/) for format conversions. All ligands were saved in .pdb format and subsequently converted to .pdbqt format using Open Babel for compatibility with the PyRx docking software. The ligand structure underwent energy minimisation to obtain the most stable conformation before docking. Docking simulations were carried out using PyRx software (version 0.8) (https://pyrx.sourceforge.io/), which implements the AutoDock Vina algorithm. A grid box of 90 E Ч 90 E Ч 90 E was set up to cover the entire protein surface and allow exhaustive sampling of binding poses. The docking was performed three times for each protein target to ensure reproducibility. Binding energies were calculated using the Lamarckian Genetic Algorithm (LGA), where more negative values indicate stronger binding affinity.

ADMET Prediction

The ADMET (Absorption, Distribution, Metabolism, Excretion, and Toxicity) predictions were conducted using two complementary software: MedChem Designer (version 5.0) and pkCSM web server (https://biosig.lab.uq.edu.au/pkcsm/) (32). To assess the drug-likeness and pharmacokinetic properties of the designed compound, *in silico* ADMET predictions were done using both sites were uploaded with a chemical structure of the C4 compound in SMILES format. The physicochemical properties such as the molecular weight, lipophilicity (LogP), hydrogen bond donors/acceptors, and breach of Lipinski rule of five that predicts oral bioavailability were evaluated using MedChem Designer. The pkCSM server made detailed forecasts of pharmacokinetic values such as intestinal absorption, blood-brain barrier penetration, interactions with the cytochrome P450 enzyme, renal elimination, and possible toxicity outcomes such as hepatotoxicity, mutagenicity, and cardiotoxicity (hERG inhibition).

MD simulations

To determine the stability of the interaction, MD simulations were performed for the as these ligands exhibited the strongest docking affinities. Simulations were conducted using the GROMOS96 53a6 force field within GROMACS (33,34). The protein–ligand complexes were solvated in a triclinic water box with a 10 Å padding and neutralized with Na^+ and Cl^- ions at a concentration of 150 mM. Energy minimization was performed using the steepest descent method until the maximum force was <1000 kJ/mol/nm (35). The system was equilibrated using the NVT ensemble for 100 ps at 300 K (V-rescale thermostat), followed by the NPT ensemble for 1 ns at 1 bar (Parrinello–Rahman barostat). Production MD simulations were carried out for 200 ns with a 2-fs time step, applying periodic boundary conditions in all directions. Hydrogen bonds were constrained with the LINCS algorithm, and long-range electrostatics were computed using the Particle Mesh Ewald method, with van der Waals and short-range electrostatics cut off at 1.0 nm. Snapshots were recorded every 10 ps for trajectory analysis (36). Root Mean Square Deviation (RMSD) and Root Mean Square Fluctuation (RMSF) analyses were conducted to evaluate structural stability. Trajectories were analyzed using GROMACS utilities. Visualization of protein–ligand interactions was performed using VMD and XM GRACE for trajectory analysis and figure generation (37).

RESULTS

Molecular Docking results

In this study, various types of PTs, including tetraphlorethols (C1), phlorethols (C2), fucophloethols (C3), pentaphloethol (C4), fucols (C5), and eckols (C6), were docked with different inflammation-related proteins: Cyclooxygenase-2, NF-κB, Interleukin-8, TNF-α, Interleukin-1β, and Interleukin-6. The binding affinities observed in the docking studies reveal the strength of interaction between each molecule and the respective protein targets in Table I and II. Among all proteins it was found that cyclooxygenase-2 (1cx2) best exhibited the overall binding affinities. The highest binding affinity of C4 with a binding energy of -9.9 kcal/mol was observed with C6 at -9.6 kcal/mol. C1 and C5 also had high binding affinity (-8.8 kcal/mol) and moderate binding affinity (-8.6 & -8.2 kcal/mol) respectively. In the case of NF-kB (4dn5), C4 again exhibited outstanding binding affinity of -9.8 kcal/mol and C1 was -9.4 kcal/mol. C6 interacted well with -8.7 kcal/mol with C5 (-8.3 kcal/mol), C3 (-7.9 kcal/mol), and C2 (-7.3 kcal/mol) and retained nanomolar levels of inhibitory capacity. TNF-α (2az5) had moderate

Table I: Molecules and Their Corresponding Names

Molecule	Name
Molecule 1 (C1)	Tetraphloroethol
Molecule 2 (C2)	Phlorethol
Molecule 3 (C3)	Fucophloethol
Molecule 4 (C4)	Pentaphloethol
Molecule 5 (C5)	Fucol
Molecule 6 (C6)	Eckol

Table II: Docking Results for Various Ligands and Molecules

Ligand	Molecule	BA (kcal/mol)	RMSD/ub	RMSD/lb	LE	IC (k*i*)
1cx2	C1	-8.8	0	0	-0.39	55.25 nM
1cx2	C2	-8.4	0	0	-0.34	78.25 nM
1cx2	C3	-8.2	0	0	-0.33	87.95 nM
1cx2	**C4**	**-9.9**	**0**	**0**	**-0.44**	**35.75 nM**
1cx2	C5	-8.6	0	0	-0.38	65.45 nM
1cx2	C6	-9.6	0	0	-0.41	48.25 nM
2az5	C1	-6.2	0	0	-0.29	122.65 nM
2az5	C2	-5.8	0	0	-0.21	25.32 µM
2az5	**C3**	**-7.4**	**0**	**0**	**-0.31**	**90.24 nM**
2az5	C4	-7	0	0	-0.30	100.24 nM
2az5	C5	-6.6	0	0	-0.26	15.24 µM
2az5	C6	-6.8	0	0	-0.28	18.26 µM
3il8	C1	-6.3	0	0	-0.23	24.35 µM
3il8	C2	-5.2	0	0	-0.19	12.5 µM
3il8	C3	-6.1	0	0	-0.21	25.32 µM
3il8	**C4**	**-7**	**0**	**0**	**-0.30**	**102.35 nM**
3il8	C5	-5.8	0	0	-0.18	54.25 µM
3il8	C6	-6.5	0	0	-0.25	14.25 µM
4dn5	C1	-9.4	0	0	-0.40	54.75 nM
4dn5	C2	-7.3	0	0	-0.31	92.35 nM
4dn5	C3	-7.9	0	0	-0.32	80.25 nM
4dn5	**C4**	**-9.8**	**0**	**0**	**-0.42**	**40.36 nM**
4dn5	C5	-8.3	0	0	-0.33	88.24 nM
4dn5	C6	-8.7	0	0	-0.38	66.25 nM
7chy	C1	-6.6	0	0	-0.26	15.47 µM
7chy	C2	-6.4	0	0	-0.24	20.47 µM
7chy	C3	-6.4	0	0	-0.24	19.25 µM
7chy	C4	-6.4	0	0	-0.24	20.17 µM
7chy	C5	-6.4	0	0	-0.24	20.37 µM
7chy	**C6**	**-7.3**	**0**	**0**	**-0.30**	**94.37 nM**
8c3u	C1	-7.2	0	0	-0.31	87.36 nM
8c3u	C2	-7	0	0	-0.30	91.34 nM
8c3u	C3	-7.6	0	0	-0.32	80.25 nM
8c3u	**C4**	**-8.6**	**0**	**0**	**-0.34**	**75.55 nM**
8c3u	C5	-7.6	0	0	-0.31	92.68 nM
8c3u	C6	-8.3	0	0	-0.33	72.36 nM

BA – Binding Affinity; RMSD - Root Mean Square Deviation; LE – Ligand Efficiency (LE is a metric used in drug discovery to measure the binding energy of a ligand per atom to a binding partner); IC – Inhibitory Constant (Predicted values from Autodock)

binding affinities to all phlorotannins. C3 demonstrated the best affinity of -7.4 kcal/mol, then C4 -7.0 kcal/mol. C6, C5, C1 and C2 had weaker binding energies lying in the range -6.8, -6.6, -5.8 & 6.2 kcal/mol. The interactions of interleukin-8 (3il8) were also relatively weak as compared to COX-2 and NF-kB. C4 exhibited the highest binding affinity with a docking score of -7.0 kcal/mol, indicating moderate to good binding potential. C6 showed the second-best affinity at -6.5 kcal/mol, followed by C1 (-6.3 kcal/mol) and C3 (-6.1 kcal/mol). The compounds C5 and C2 demonstrated lower binding affinities of -5.8 kcal/mol and -5.2 kcal/mol, respectively, suggesting weaker interactions with the IL-8 binding site.

All phlorotannins had rather similar but moderate binding affinities with Interleukin-1β (7chy). C6 had the highest interaction which was -7.3 kcal/mol with C1, C2, C3, C4 and C5 showing comparable binding energies of -6.6 to -6.4 kcal/mol. The Interleukin-6 (8c3u) was showing moderate binding with all the compounds. C4 best exhibited the affinity at -8.6 kcal/mol and C6 at -8.3 kcal/mol. C3 and C5 both had a binding energy of -7.6 kcal/mol, whereas the binding energy of C1 (-7.2 kcal/mol) and C2 (-7.0 kcal/mol) was slightly lower. In general, the docking outcomes indicated that C4 (pentaphloethol) had a consistently high binding affinity to all six targets of inflammatory proteins but was most effective against COX-2 (-9.9 kcal/mol) and NF-kappa B (-9.8 kcal/mol).

CONTINUE

Cyclooxygenase-2 and NF-κB were selected for further detailed molecular interaction studies based on their strongest binding affinities with C4, aiming to elucidate the structural mechanisms responsible for the compound's anti-inflammatory potential. The interaction of C4 with the cyclooxygenase-2 protein was further analyzed and visualized through various panels, providing a detailed understanding of the binding mechanism. The C4-cyclooxygenase-2 complex, Figure 1A,B) was located in the depth of the active site and surrounded by polar and hydrophobic residues. This ligand made several typical hydrogen bonds with ASN43, TYR123, ARG61, GLU46, ASP58, SER126 and ARG469 besides and Pi-alkyl interactions between ARG44. The complex was further stabilized by Van der Waals contacts with residues like PHE, LYS, THR, ASP and PHE. Heavy hydrogen-bond network and hydrophobic packing indicate that the interaction pattern is strong and specific that could help in the inhibition of 1cx2 activity. In the NfkB-C4 complex (Figure 1C,D), the ligand had transitioned into a surface-binding pocket made up of nonpolar and polar residues. The strong hydrogen bonds were found at SER410, GLY409 and GLY412 whereas the electrostatic complementarity was increased by Pi-alkyl interactions including LYS482, LEU406, VAL414, LEU522. The aromatic regions of C4 of the binding groove were stabilized by hydrophobic interactions with LEU, GLU, LYS, ARG, CYS, ASP, GLY and MET residues. The observed pattern of contact demonstrates that C4 might disrupt the TNF-alpha receptor-binding interface or oligomeric stability. In comparison, a deeper active and compact binding pose in C4 to cyclooxygenase-2, suggested a higher likely stability, whereas the ligand in TNF-α was extended across the surface interface, which may suggest the ability to modulate protein-protein interactions.

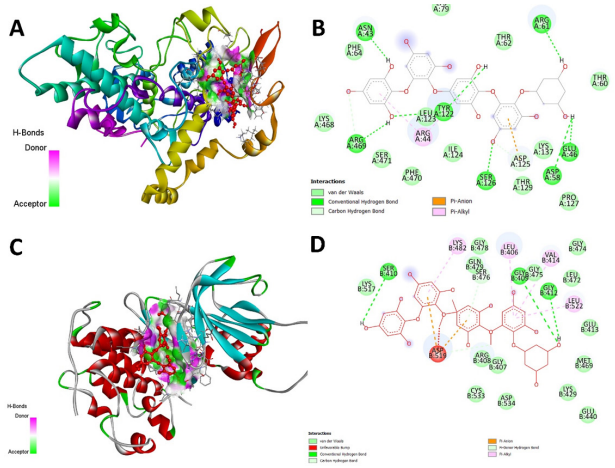

Figure 1: Molecular interaction of compound C4 with inflammatory targets. (A) 3D structure of the cyclooxygenase protein complexed with C4, showing the ligand bound within the active site. (B) 2D interaction diagram of C4–cyclooxygenase complex illustrating van der Waals forces, hydrogen bonds, Pi-anion, and Pi-alkyl interactions. (C) 3D structure of TNF-α complexed with C4, highlighting the binding pocket and hydrogen-bond network. (D) 2D interaction diagram of the C4–TNF-α complex showing key van der Waals and hydrogen-bond interactions stabilizing the ligand within the active site.

ADMET Profiling of Compound C4 Using pkCSM and MedChem Designer

The pkCSM-based *in silico* analysis of compound C4 is summarized in Table III. The C4 showed moderate aqueous solubility (–2.892 log mol/L) and a borderline Caco-2 permeability value (–0.253 log Papp in 10^{-6} cm/s). Although C4 was predicted to have a high human intestinal absorption rate of 76.09%, this suggests that oral delivery could be feasible. Skin permeability was very low (–2.735 log Kp), indicating poor transdermal uptake. Interestingly, C4 was predicted as a substrate of P-glycoprotein, which may limit intracellular accumulation through efflux.

The predicted value of steady-state volume of distribution (VDss) was low (–0.022 log L/kg), indicating that the

Table III: Predicted ADMET Properties of Pentaphloethol

Property	Model Name	Predicted Value	Unit
Absorption	Water solubility	**-2.892**	Numeric (log mol/L)
Absorption	Caco2 permeability	**-0.253**	Numeric (log Papp in 10^{-6} cm/s)
Absorption	Intestinal absorption (human)	**76.094**	Numeric (% Absorbed)
Absorption	Skin Permeability	**-2.735**	Numeric (log Kp)
Absorption	P-glycoprotein substrate	**Yes**	Categorical (Yes/No)
Absorption	P-glycoprotein I inhibitor	**No**	Categorical (Yes/No)
Absorption	P-glycoprotein II inhibitor	**Yes**	Categorical (Yes/No)
Distribution	VDss (human)	**-0.022**	Numeric (log L/kg)
Distribution	Fraction unbound (human)	**0.383**	Numeric (Fu)
Distribution	BBB permeability	**-2.975**	Numeric (log BB)
Distribution	CNS permeability	**-4.621**	Numeric (log PS)
Metabolism	CYP2D6 substrate	**No**	Categorical (Yes/No)
Metabolism	CYP3A4 substrate	**No**	Categorical (Yes/No)
Metabolism	CYP1A2 inhibitor	**No**	Categorical (Yes/No)
Metabolism	CYP2C19 inhibitor	**No**	Categorical (Yes/No)
Metabolism	CYP2C9 inhibitor	**No**	Categorical (Yes/No)
Metabolism	CYP2D6 inhibitor	**No**	Categorical (Yes/No)
Metabolism	CYP3A4 inhibitor	**No**	Categorical (Yes/No)
Excretion	Total Clearance	**0.713**	Numeric (log ml/min/kg)
Excretion	Renal OCT2 substrate	**No**	Categorical (Yes/No)
Toxicity	AMES toxicity	**No**	Categorical (Yes/No)
Toxicity	Max. tolerated dose (human)	**0.438**	Numeric (log mg/kg/day)
Toxicity	hERG I inhibitor	**No**	Categorical (Yes/No)
Toxicity	hERG II inhibitor	**Yes**	Categorical (Yes/No)
Toxicity	Oral Rat Acute Toxicity (LD50)	**2.482**	Numeric (mol/kg)
Toxicity	Oral Rat Chronic Toxicity (LOAEL)	**6.637**	Numeric (log mg/kg_bw/day)
Toxicity	Hepatotoxicity	**No**	Categorical (Yes/No)
Toxicity	Skin Sensitisation	**No**	Categorical (Yes/No)
Toxicity	*T.Pyriformis* toxicity	**0.285**	Numeric (log ug/L)
Toxicity	Minnow toxicity	**1.54**	Numeric (log mM)

penetration across the tissues was low, and plasma distribution preferred. The proportion of unbound in the plasma was determined to be 0.383, which is in line with moderate protein binding. Both blood-brain barrier penetration (–2.975) and CNS permeability (-4.621) were modelled to be ineffective meaning that there is low central effects and low risk of neurotoxicity. Such predictions showed that C4 does not act as a substrate or inhibitor of major isoforms (CYP3A4, CYP2D6, CYP1A2, CYP2C19, CYP2C9) of CYP450. The predicted clearance of the compound was 0.713 log ml/min/kg, which is in line with the moderate rate of elimination. It was found that the C4 was not a substrate of renal OCT2 transporter, indicating that the kidney clearance was not the main elimination pathway. The total toxicity estimates were optimal. Moreover, C4 was not mutagenic (Ames test) or hepatotoxic or skin sensitizing. The highest dose that could be tolerated by humans was approximated as 0.438 logmg/kg/day. The highest predicted value of acute oral toxicity in rats was 2.482 mol/kg and chronic toxicity (LOAEL) was 6.637 log mg/kg bw/day, which is in an acceptable range. The possible concern was identified as hERG II channel inhibition which should be followed by additional examination of the *in vitro* cardiotoxicity. Predictions of environmental toxicity showed moderate ecotoxicity with Tetrahymena pyriformis toxicity of 0.285 log μg/L and minnow toxicity of 1.54 log mM which, despite this, indicate that ecotoxicity could be manageable.

MD Simulations

MD simulations of 200 ns were done to determine the dynamic stability and conformational behaviour of the C4 complexes with COX-2. The overall system stability and the flexibility of the residues were measured using the root mean square deviation (RMSD), root mean square fluctuation (RMSF), and hydrogen bonds (H-bonds) analysis (Fig. 2) respectively. The RMSD profiles (Fig. 2A) indicated that the apo-protein (COX-2) and the C4 ligand-bound complexes reached equilibrium within the first 50 ns of the simulation, and then stayed at equilibrium throughout the 200 ns production simulation. The values of the average RMSD of the apo-protein and protein-ligand complex were found to be around 0.30 nm and 0.35 0.38 nm, respectively. Even though the ligand-complexed systems had a slightly larger RMSD than the apo-protein, the deviations were within the acceptable range (less than 0.4 nm), which suggests no severe structural disturbances. This is an indication that the binding of the ligand does not alter the protein conformation but stabilizes the complex into a dynamic equilibrium position. The regular trends of RMSD validate the stability of docking queries and the entire stability of the simulated systems. The RMSF analysis (Fig. 2B) indicated that the patterns of fluctuation of the apo and complexed proteins are similar with the majority of the residues having RMSFD values of less than 0.25 nm. Increased flexibility was found in loop regions and at the terminal residue but the secondary structural elements (alpha-helices and beta-sheets) were preserved. There were less fluctuations in key active-site residues in the ligand-bound complexes, which indicates that ligand binding can limit local conformational mobility and add to a more rigid structure of the binding pocket. All these results suggest that the C4 complexes with COX-2 are dynamically stable and retain their conformational integrity throughout the 200ns simulation, which allows the strong binding affinity in molecular docking to be supported.

The profile of temporal variation in the number of hydrogen bonds formed between the C4 ligand and COX-2 (Fig. 2C) illustrates how the number of hydrogen bonds varied within the 200 ns period of the molecular dynamics simulation. The H-bonds varied in number (ranging between 1 and 8) along the trajectory, with an average of approximately 3-4 bonds being preserved throughout the trajectory. This represents a steady and dynamic contact pattern among the active-site residues and the ligand. The periodic changes in the number of hydrogen bonds indicate that there are temporary interactions which facilitate stabilization of the complex at various conformational states. The constant existence of numerous H-bonds during the simulation continues to affirm that the ligand did not separate or destabilize out of the binding pocket.

The hydrogen bond occupancy analysis (Fig. 2D) gives more in-depth information about the intermolecular interactions that stabilize the C4 COX-2 complex throughout the 200 ns simulation. The C4 ligand was found to have several hydrogen bonds with essential active-site residues, which showed a steady and selective binding profile. CYS37 exhibited the greatest

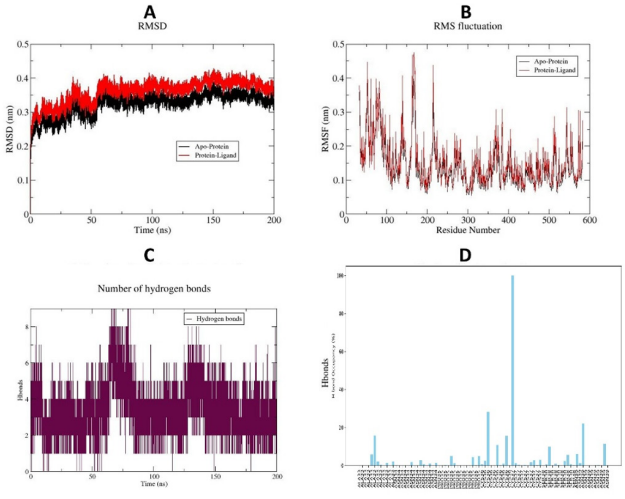

Figure 2: Molecular dynamics (MD) simulation analysis of the C4–COX-2 complex over 200 ns. (A) Root mean square deviation (RMSD) plot showing the structural stability of the apo-protein (black) and protein–ligand complex (red). (B) Root mean square fluctuation (RMSF) plot illustrating residue-level flexibility. (C) Time evolution of hydrogen bonds formed between the ligand and protein during the 200 ns trajectory. (D) Hydrogen bond occupancy plot showing the percentage of interaction persistence for each residue.

hydrogen bond cover (nearly 100 %) indicating that the interaction was solid and maintained over 200 ns. Other residues like ASN38, ASN39, ALA33, and PRO35 were forming transient hydrogen bonds with occupancy of 10-30% which helped in the dynamic stabilization of the complex. The binding pocket is anchored by a strong and persistent hydrogen bond between C4 and CYS37, which is likely to keep the ligand in the preferred orientation. The additional binding with residues like ASN38, ASN39, ALA33 and PRO35 further enhance the structural integrity of the binding site and inhibit the drift in the conformations. Overall, the hydrogen-bonding profile supports the structural stability and dynamic equilibrium of the simulated complex, reflecting a well-maintained intermolecular interaction network throughout the 200 ns production run.

Physicochemical and Drug-Likeness Evaluation

The physicochemical properties of the PTs studied showed important variations depending on the different molecular structure, that has important consequences for their pharmaceutical potential (Table IV). Analysis of the lipophilicity parameter revealed that C2 had the highest potential of membrane permeability with DiffCoe_P value of 0.917, followed by C5 (0.741) and C3 (0.731). In contrast, C1 and C4 showed moderate lipophilicity values of 0.621 and 0.547, respectively. The Mlog P values also supported these trends with C2 displaying a positive value of 0.358, whereas Mlog P for C3 displayed an unusual negative value of -0.6 suggesting an increased hydrophilic character. Solubility predictions as indicated by the S+log P and S+log D values showed critical differences among the compounds. C1 (3.612/3.162), C4 (3.086/4.674), and C6 (4.275/3.699) had problematic solubility profiles that may reduce their bioavailability. Conversely, C5 (1.823/1.722), C3 (1.871/1.683) and C2 (1.326/1.077) showed more favourable solubility characteristics. These results imply the importance of the lower molecular weight phlorotannins in having better aqueous solubility, which is crucial in absorption and distribution in biological systems.

Evaluation of the drug-likeness by Lipinski's Rule of Five showed that C2 was the only compound having zero violations, suggesting optimum oral bioavailability potential. C5 and C3 each broke one rule, largely because of hydrogen bonding capacity (Hb); while having acceptable molecular weights of 358.30 and 374.30 Da, respectively. In contrast, C1, C4 and C6 violated two to three rules, with the most important being high molecular weights (498.40, 622.49, and 510.41 Da), too many hydrogen bond donors and acceptors, and high topological polar surface areas. The molecular weight displayed a progressive increase from C2 (250.20 Da) to C4 (622.49 Da) being correlated with the reduction of drug-likeness scores.The topological polar surface area (T_PS_A) values ranged from 110.38 E for C2 to 259.45 E for C4. Compounds with T_PS_A values exceeding 140 E typically exhibit reduced membrane permeability, which was observed for C1 (209.76 E), C4 (259.45 E), and C6 (213.67 E). The number of hydrogen bond donors (HBD_H) increased from 5 in C2 to 11 in C4, while nitrogen and oxygen atoms (M_NO) ranged from 6 to 15, reflecting the structural complexity of higher oligomers. These parameters taken together indicate the decreasing permeability of the membranes to the flow with the increasing degree of polymerization. The results provide an inverse relationship between structural complexity and pharmaceutical accessibility. Smaller phlorotannin units, especially C2 and C5, showed better drug-like properties including favourable lipophilicity, solubility and molecular weight characteristics. Larger oligomeric structures that may still have improved biological activities are facing substantial challenges of oral bioavailability and cellular uptake.

DISCUSSION

The docking results showed that these PTs, especially pentaphloethol (C4) have the highest binding affinities in the series of PTs used in the present study for stable interaction with the critical inflammatory cytokines such as NF-kB and COX-2. These findings are consistent with those reported on the polyphenols derived from marine sources, which have demonstrated the capacity to inhibit inflammatory signalling pathways and to decrease the action of cytokines (38). The strong binding affinity and stable molecular interactions observed for C4 highlight its potential as an anti-inflammatory lead molecule.

The pharmacokinetic predictions for C4 revealed favourable absorption and low toxicity, while the possibility of CYP mediated interactions was low,

Table IV: Physicochemical Properties of PTs

Name	DiffCoef	MlogP	S+logP	S+logD	RuleOf5	Rule of 5_Code	MWt	M_NO	T_PSA	HBDH
Tetraphloroethol	0.621	-1.661	3.612	3.162	2	Hb; NO	498.403	12	209.76	9
Phlorethol	0.917	0.358	1.326	1.077	0	<None>	250.209	6	110.38	5
Fucophloethol	0.731	-0.6	1.871	1.683	1	Hb	374.306	9	171.07	8
Pentaphloethol	0.547	-2.785	5.086	4.674	3	Hb; Mw; NO	622.499	15	259.45	11
Fucol	0.741	0.139	1.823	1.722	1	Hb	358.307	8	161.84	8
Eckol	0.621	-1.915	4.275	3.699	3	Hb; Mw; NO	510.414	12	213.67	9

S + log D - log D at user-specified pH (default 7.4), based on S + log P. **MlogP** - Moriguchi estimation of log P. **HBDH** - Number of Hydrogen bond donor protons. **M_NO** - Total number of Nitrogen and Oxygen atoms. **T_PSA** - Topological polar surface area in square angstroms. **RuleOf5** - Lipinski's Rule of Five: a score indicating the number of potential problems a structure might have with passive oral absorption. RuleOf5_Code - Lipinski's Rule of Five codes: LP = log P; Hb = number of Hydrogen bond donor protons; Mw = molecular weight; NO = number of Nitrogen- and Oxygen-based Hydrogen bond acceptors.

suggesting that the compound is suitable for systemic administration. Although C4 showed the violation of some parameters of Lipinski's rule, especially because of its high molecular weight (622.49 Da) and the high number of hydrogen-bond donors (HBDH = 11) values, these are normal for natural polyphenols and do not prevent bioactivity. Many clinically relevant marine-derived compounds, such as eckol and dieckol, exceed these limits but exhibit therapeutic potential through mechanisms such as transport-mediated uptake, facilitated diffusion or metabolic conversion of compounds into more permeable derivatives (39). Therefore, in spite of these violations of the rules, the overall data of ADMET and pkCSM supports the drug-like behaviour of C4.

The detailed analysis of the protein-ligand interaction gives mechanistic insight into the anti-inflammatory potential of C4. Within the COX-2 binding pocket, C4 made stable hydrogen bonds with Tyr385, Ser530 and Arg120, residues that are essential for substrate binding and catalytic activity. These interactions probably interfere with the access of arachidonic acid to the catalytic site and thus decrease prostaglandins synthesis and inflammatory response. Similarly, in the NF-kB complex, C4 was involved in hydrogen bonding and pi-pi stacking with residues such as Lys221, Glu223 and Arg246, stabilizing the complex and potentially preventing NF-kB from binding to DNA promoter regions. Such inhibition could inhibit downstream transcription of pro-inflammatory cytokines such as IL-1β, IL-6, and TNF-α. Comparable residue level interactions have been reported with other marine polyphenols like eckol and dieckol which inhibit COX-2 and NF-kB via similar hydrogen bonding to Tyr385 and Glu223, respectively (40–44). These findings indicate that structural features such as hydroxyl-rich aromatic rings play a central role in protein pocket stabilization and pathway modulation. The 200ns MD simulations of the COX-2-C4 complex were also performed to further evaluate the stability and dynamic behaviour of the complex. It was observed that the mean values of RMSD were below 0.2 nm over the 200ns time range, which showed that there was low conformational movement and high stability of the complex. The scale of these low RMSD deviations suggests that C4 is in regular contact with active-site residues, which suggests structural rigidity and retains the potential to be inhibitory. Investigations of MD simulation activity have identified stable RMSD deviations and smaller RMSF deviations as distinguishing features of effective inhibitors that cause longer-term binding and functional inhibition of target proteins (45). Therefore, the constant level of C4 under the influence of COX-2 confirms its structural compatibility and drug applicability.

The general ADMET characteristics indicates that the C4 compound would have a reasonable exposure to the system, intestinal absorption and moderate plasma distribution after the compound is taken orally. Even though transdermal uptake seems to be limited, this is in line with the hydrophilic and polyphenolic nature of the compound, which prefers the oral pathways of delivery (46). The estimated interaction with P-glycoprotein shows that efflux transport has the potential of affecting intracellular accumulation but this is inhibited partially by P-gp II as an indication of a self-regulatory mechanism that may maintain therapeutic levels of the drug in the cell (47). The lack of major CYP450 activity as a substrate or inhibitor indicates a very low probability of metabolic drug-drug interactions, a critical benefit to the long-term use of anti-inflammatory therapy (48). The toxicological profile indicates that C4 safety profile. Non-mutagenic and non-hepatotoxic predictions are consistent with established properties of marine-derived phlorotannins which typically have low systemic toxicity and excellent biocompatibility (49). The low CNS penetration also implies the low potential of neurotoxicity and the moderate nature of clearance indicates that the exposure to systems is not readily eliminated (50). Overall, the findings highlight C4 as a promising marine-derived compound for an anti-inflammatory drug. Its capacity to modulate multiple cytokine targets, combined with promising pharmacokinetic characteristics, positions it as a potential for future preclinical investigations. Experimental validation, including *in vitro* and *in vivo* studies, will be crucial to confirm these *in silico* findings and advance the development of C4 as a therapeutic candidate for inflammation-mediated disorders.

CONCLUSION

This *in silico* study has found pentaphloethol (C4) as a good therapeutic lead with high anti-inflammatory ability. Among the phlorotannins (PTs) tested, the compound C4 has the highest binding affinities to the important cytokine targets including NF-κB and COX-2 . The therapeutic potential of this compound is supported by its significant ADMET properties 76.094% human intestinal absorption and low toxicity risks, although it has violated the Lipinski rule to some degree. The C4 protein-ligand interactions were found to be stable as confirmed by the use of molecular dynamics simulations with minimal conformational change. Complementary pharmacokinetic predictions revealed a favorable ADMET profile, characterized by optimal absorption, metabolic stability, and low predicted toxicity. Although C4 shows minor deviations from Lipinski's rule, these features are characteristic of polyphenolic natural products. Overall, the integrated computational analysis highlights C4 as a promising marine-derived anti-inflammatory candidate that warrants further experimental validation through *in vitro* and *in vivo* studies.

ACKNOWLEDGEMENT

The authors of this article would like to acknowledge

the technical support provided by Saveetha Institute of Medical and Technical Sciences, Saveetha University, Chennai, 600 077, Tamil Nadu, India.

REFERENCES

1. Bennett JM, Reeves G, Billman GE, Sturmberg JP. Inflammation–Nature's Way to Efficiently Respond to All Types of Challenges: Implications for Understanding and Managing "the Epidemic" of Chronic Diseases. Front Med [Internet]. 2018 Nov 27 [cited 2024 Dec 3];5. Available from: https://www.frontiersin.org/journals/medicine/articles/10.3389/fmed.2018.00316/full
2. Furman D, Campisi J, Verdin E, Carrera-Bastos P, Targ S, Franceschi C, et al. Chronic inflammation in the etiology of disease across the life span. Nat Med. 2019 Dec;25(12):1822–32.
3. Kany S, Vollrath JT, Relja B. Cytokines in Inflammatory Disease. Int J Mol Sci. 2019 Nov 28;20(23):6008.
4. Megha KB, Joseph X, Akhil V, Mohanan PV. Cascade of immune mechanism and consequences of inflammatory disorders. Phytomedicine. 2021 Oct;91:153712.
5. Liu T, Zhang L, Joo D, Sun SC. NF-κB signaling in inflammation. Signal Transduct Target Ther. 2017 July 14;2:17023.
6. Blobaum AL, Marnett LJ. Structural and Functional Basis of Cyclooxygenase Inhibition. J Med Chem. 2007 Apr 1;50(7):1425–41.
7. Jang D in, Lee AH, Shin HY, Song HR, Park JH, Kang TB, et al. The Role of Tumor Necrosis Factor Alpha (TNF-α) in Autoimmune Disease and Current TNF-α Inhibitors in Therapeutics. Int J Mol Sci. 2021 Mar 8;22(5):2719.
8. Bhol NK, Bhanjadeo MM, Singh AK, Dash UC, Ojha RR, Majhi S, et al. The interplay between cytokines, inflammation, and antioxidants: mechanistic insights and therapeutic potentials of various antioxidants and anti-cytokine compounds. Biomedicine & Pharmacotherapy. 2024 Sept 1;178:117177.
9. Cabral-Pacheco GA, Garza-Veloz I, Castruita-De la Rosa C, Ramirez-Acuca JM, Perez-Romero BA, Guerrero-Rodriguez JF, et al. The Roles of Matrix Metalloproteinases and Their Inhibitors in Human Diseases. Int J Mol Sci. 2020 Dec 20;21(24):9739.
10. Taylor EB, Hall JE, Mouton AJ. Current anti-inflammatory strategies for treatment of heart failure: From innate to adaptive immunity. Pharmacological Research. 2025 June 1;216:107761.
11. Sokolowska M, Rovati GE, Diamant Z, Untersmayr E, Schwarze J, Lukasik Z, et al. Effects of non-steroidal anti-inflammatory drugs and other eicosanoid pathway modifiers on antiviral and allergic responses: EAACI task force on eicosanoids consensus report in times of COVID-19. Allergy. 2022;77(8):2337–54.
12. Rao PPN, Kabir SN, Mohamed T. Nonsteroidal Anti-Inflammatory Drugs (NSAIDs): Progress in Small Molecule Drug Development. Pharmaceuticals. 2010 May;3(5):1530–49.
13. Al-Saeed A. Gastrointestinal and Cardiovascular Risk of Nonsteroidal Anti-inflammatory Drugs. Oman Med J. 2011 Nov;26(6):385–91.
14. Coutinho AE, Chapman KE. The anti-inflammatory and immunosuppressive effects of glucocorticoids, recent developments and mechanistic insights. Molecular and Cellular Endocrinology. 2011 Mar 15;335(1):2–13.
15. Sharma Y, Arora M, Bala K. The potential of immunomodulators in shaping the future of healthcare. Discov Med. 2024 Sept 3;1(1):37.
16. Dash UC, Nayak V, Navani HS, Samal RR, Agrawal P, Singh AK, et al. Understanding the molecular bridges between the drugs and immune cell. Pharmacology & Therapeutics. 2025 Mar 1;267:108805.
17. Dhanabalan AK, Vasudevan S, Velmurugan D, Khan MS. Identification of potential marine bioactive compounds from brown seaweeds towards BACE1 inhibitors: molecular docking and molecular dynamics simulations approach. *in silico* Pharmacol. 2024 May 6;12(1):40.
18. Maheswari V, Babu PAS. Comprehensive reviews on phenolic compounds from Phaeophyceae as potential therapeutic agent. J App Biol biotech. 2022 July 20;14–21.
19. Pйrez M, Falquй E, Domнnguez H. Antimicrobial Action of Compounds from Marine Seaweed. Marine Drugs. 2016 Mar 9;14(3):52.
20. Mukherjee A, Das B. The role of inflammatory mediators and matrix metalloproteinases (MMPs) in the progression of osteoarthritis. Biomaterials and Biosystems. 2024 Mar 1;13:100090.
21. Li Z, Huang Z, Zhang H, Lu J, Tian Y, Wei Y, et al. P2X7 Receptor Induces Pyroptotic Inflammation and Cartilage Degradation in Osteoarthritis via NF-κ B/NLRP3 Crosstalk. Persichini T, editor. Oxidative Medicine and Cellular Longevity. 2021 Jan;2021(1):8868361.
22. Besednova NN, Andryukov BG, Zaporozhets TS, Kuznetsova TA, Kryzhanovsky SP, Ermakova SP, et al. Molecular Targets of Brown Algae Phlorotannins for the Therapy of Inflammatory Processes of Various Origins. Mar Drugs. 2022 Mar 30;20(4):243.
23. Nasiri M, Langarizadeh MA, Aghilinasab A, Amani A, Ranjbar Tavakoli M, Sharififar F. Phlorotannins as Marine-Derived Polyphenols for Advancing Cosmeceutical Formulations. Chemistry & Biodiversity. n/a(n/a):e00188.
24. Herath KHINM, Nagahawatta DP, Wang L, Sanjeewa KKA. The Role of Phlorotannins to Treat Inflammatory Diseases. Chemistry. 2025 May 4;7(3):77.
25. Nyijime TA, Shallangwa GA, Uzairu A, Umar AB,

Ibrahim MT, Madkhali HA, et al. Computational design, pharmacokinetics, molecular docking and molecular dynamic simulation of novel anti-tubercular inhibitors. *In Silico* Research in Biomedicine. 2025 Jan 1;1:100012.
26. Meunier M, Schinkovitz A, Derbré S. Current and emerging tools and strategies for the identification of bioactive natural products in complex mixtures. Nat Prod Rep. 2024 Nov 13;41(11):1766–86.
27. Samy S, Alagumuthu M, Dangate MS. Antimicrobial effects of new tetrahydrofurans. European Journal of Medicinal Chemistry Reports. 2024 Dec;12:100191.
28. Manikandan A, Jeevitha S, Vusa L. Peptidomimetics for CVD screened via TRADD-TRAF2 complex interface assessments. *In Silico* Pharmacol. 2023 Oct 27;11(1):28.
29. Alagumuthu M, Rajpoot S, Baig MS. Structure-Based Design of Novel Peptidomimetics Targeting the SARS-CoV-2 Spike Protein. Cel Mol Bioeng. 2021 Apr 1;14(2):177–85.
30. Shenoy A, Maiti S, Jayaram S, yadalam P kumar, Paulraj J. Assessing the role of PEKK implant material on cytotoxicity, inflammatory response, and molecular interactions with pro-inflammatory cytokines: An in-vitro and in-silico study. Journal of Oral Biology and Craniofacial Research. 2025 Nov 1;15(6):1218–23.
31. Natarajan SR, Krishnamoorthy R, Alshuniaber MA, Alsulami TS, Gatasheh MK, Rajagopal P, et al. ABCE1 facilitates tumour progression via aerobic glycolysis and inhibits cell death in human colorectal cancer cells through the p53 signalling pathway. Sci Rep. 2025 July 9;15(1):24674.
32. Velmurugan Y, Chakkarapani N, Natarajan SR, Jayaraman S, Madhukar H, Venkatachalam R. PPI networking, in-vitro expression analysis, virtual screening, DFT, and molecular dynamics for identifying natural TNF-□ inhibitors for rheumatoid arthritis. Mol Divers [Internet]. 2025 Apr 19 [cited 2025 Oct 8]; Available from: https://doi.org/10.1007/s11030-025-11158-x
33. Durrant JD, McCammon JA. Molecular dynamics simulations and drug discovery. BMC Biol. 2011 Oct 28;9:71.
34. Vemula V, Marudamuthu AS, Prasad S, B M S, S E M, A S, et al. Fragment-based design and MD simulations of human papilloma virus-16 E6 protein inhibitors. J Biomol Struct Dyn. 2024;42(1):288–97.
35. Oostenbrink C, Villa A, Mark AE, Van Gunsteren WF. A biomolecular force field based on the free enthalpy of hydration and solvation: The GROMOS force-field parameter sets 53A5 and 53A6. Journal of Computational Chemistry. 2004;25(13):1656–76.
36. Gladies Raymond Mohanraj D, Alagumuthu M, Chellam S, Suresh Kumar A, Nagaraj Poojari T, Suresh Kumar J, et al. EGFR Kinase Inhibiting Amino-enones for Breast Cancer; CADD Approach. Curr Comput Aided Drug Des. 2024 Jan 30;
37. S J, A M, P P, G R. Anticandidal Effect of New Imidazole Derivatives Over Aspartic Protease Inhibition. Chem Biodivers. 2024 Jan;21(1):e202301276.
38. Pereira L, Cotas J. Therapeutic Potential of Polyphenols and Other Micronutrients of Marine Origin. Mar Drugs. 2023 May 26;21(6):323.
39. Hu L, Luo Y, Yang J, Cheng C. Botanical Flavonoids: Efficacy, Absorption, Metabolism and Advanced Pharmaceutical Technology for Improving Bioavailability. Molecules. 2025 Mar 6;30(5):1184.
40. Kraiem M, Ben Hamouda S, Eleroui M, Ajala M, Feki A, Dghim A, et al. Anti-Inflammatory and Immunomodulatory Properties of a Crude Polysaccharide Derived from Green Seaweed Halimeda tuna: Computational and Experimental Evidences. Marine Drugs. 2024 Feb;22(2):85.
41. Owczarek K, Lewandowska U. The Impact of Dietary Polyphenols on COX-2 Expression in Colorectal Cancer. Nutrition and Cancer. 2017 Nov 17;69(8):1105–18.
42. Dos Santos Nascimento IJ, Da Silva-Jьnior EF. TNF-α Inhibitors from Natural Compounds: An Overview, CADD Approaches, and their Exploration for Anti-inflammatory Agents. CCHTS. 2022 Dec;25(14):2317–40.
43. Smith WL, Urade Y, Jakobsson PJ. Enzymes of the Cyclooxygenase Pathways of Prostanoid Biosynthesis. Chem Rev. 2011 Oct 12;111(10):5821–65.
44. Vecchio AJ, Simmons DM, Malkowski MG. Structural Basis of Fatty Acid Substrate Binding to Cyclooxygenase-2. J Biol Chem. 2010 July 16;285(29):22152–63.
45. Balachandran P, Parthasarathy V, Ajay Kumar TV. Isolation of Compounds from Sargassum wightii by GCMS and the Molecular Docking against Anti-Inflammatory Marker COX2. ILCPA. 2016 Jan 4;63:1–12.
46. Schafer N, Balwierz R, Biernat P, Ochędzan-Siodłak W, Lipok J. Natural Ingredients of Transdermal Drug Delivery Systems as Permeation Enhancers of Active Substances through the Stratum Corneum. Mol Pharmaceutics. 2023 July 3;20(7):3278–97.
47. Nguyen TTL, Duong VA, Maeng HJ. Pharmaceutical Formulations with P-Glycoprotein Inhibitory Effect as Promising Approaches for Enhancing Oral Drug Absorption and Bioavailability. Pharmaceutics. 2021 July 20;13(7):1103.
48. Deodhar M, Al Rihani SB, Arwood MJ, Darakjian L, Dow P, Turgeon J, et al. Mechanisms of CYP450 Inhibition: Understanding Drug-Drug Interactions Due to Mechanism-Based Inhibition in Clinical Practice. Pharmaceutics. 2020 Sept 4;12(9):846.
49. Khan F, Jeong GJ, Khan MSA, Tabassum N, Kim YM. Seaweed-Derived Phlorotannins: A Review of

Multiple Biological Roles and Action Mechanisms. Mar Drugs. 2022 June 8;20(6):384.
50. Neumaier F, Zlatopolskiy BD, Neumaier B. Drug Penetration into the Central Nervous System: Pharmacokinetic Concepts and In Vitro Model Systems. Pharmaceutics. 2021 Sept 23;13(10):1542.